Clim Dyn (2006) 27:727–741
DOI 10.1007/s00382-006-0162-4

Simulations of anthropogenic change in the strength of the Brewer–Dobson circulation

N. Butchart · A. A. Scaife · M. Bourqui · J. de Grandpré · S. H. E. Hare · J. Kettleborough · U. Langematz · E. Manzini · F. Sassi · K. Shibata · D. Shindell · M. Sigmond

Received: 15 November 2005 / Accepted: 20 May 2006 / Published online: 16 August 2006

Abstract The effect of climate change on the Brewer–Dobson circulation and, in particular, the large-scale seasonal-mean transport between the troposphere and stratosphere is compared in a number of middle atmosphere general circulation models. All the models reproduce the observed upwelling across the tropical tropopause balanced by downwelling in the extra tropics, though the seasonal cycle in upwelling in some models is more semi-annual than annual. All the models also consistently predict an increase in the mass exchange rate in response to growing greenhouse gas concentrations, irrespective of whether or not the model includes interactive ozone chemistry. The mean trend is 11 kt s^{-1} $year^{-1}$ or about 2% per decade but varies considerably between models. In all but one of the models the increase in mass exchange occurs throughout the year though, generally, the trend is larger during the boreal winter. On average, more than 60% of the *mean* mass fluxes can be explained by the EP-flux divergence using the downward control principle. Trends in the annual mean mass fluxes derived from the EP-flux divergence also explain about 60% of the trend in the troposphere-to-stratosphere mass exchange rate when averaged over all the models. Apart from two models the interannual variability in the downward control derived and actual mass fluxes were generally well correlated, for the annual mean.

1 Introduction

The Brewer–Dobson circulation is a global-scale cell in the stratosphere in which air rises in the tropics and

N. Butchart (✉)
Met Office, FitzRoy Road,
Exeter, Devon EX1 3PB, UK
e-mail: neal.butchart@metoffice.gov.uk

A. A. Scaife
Hadley Centre, Met Office,
Exeter, UK

M. Bourqui · S. H. E. Hare
Department of Meteorology,
University of Reading, Reading, UK

J. de Grandpré · M. Bourqui
McGill University, Montreal, Canada

J. Kettleborough
Rutherford Laboratory,
British Atmospheric Data Centre,
Didcot, UK

U. Langematz
Freie Universität of Berlin, Berlin, Germany

E. Manzini
National Institute for Geophysics and Volcanology,
Bologna, Italy

F. Sassi
National Center for Atmospheric Research,
Boulder, CO, USA

K. Shibata
Meteorological Research Institute, Tsukuba, Japan

D. Shindell
NASA-Goddard Institute for Space Studies,
New York, USA

M. Sigmond
University of Toronto, Toronto, Canada

then moves polewards and downwards, mostly in the winter hemisphere. It was first proposed by Brewer (1949) and Dobson (1956) to explain water vapour and ozone measurements and is now generally accepted as the basic description of the seasonal-mean meridional mass transport in the stratosphere. It is thought to be driven by dissipation of Rossby and gravity wave pseudomomentum fluxes from the troposphere (e.g., Holton et al. 1995). The main refinement to this simple picture of an overturning circulation is the addition of quasi-horizontal mixing due to mid-latitude planetary waves breaking.

In the tropics the strength of the Brewer–Dobson circulation sets the rate at which air is transported from the tropical-tropopause-layer into the stratosphere. Consequently, for example, it almost completely determines the timescale for the removal of chlorofluorcarbons (CFCs) from the atmosphere as these have no significant tropospheric removal process but are rapidly photolyzed above the ozone peak. Using a middle atmosphere general circulation model (GCM) Butchart and Scaife (2001) predicted that climate change from increasing amounts of CO_2 will increase the troposphere–stratosphere mass exchange by 3% per decade and thereby reduce the lifetimes of CFCs at a similar rate. Similarly, Rind et al. (2001) estimated a 30% increase in the troposphere-to-stratosphere mass flux due to a doubling of CO_2 concentrations.

Both Butchart and Scaife (2001), and Rind et al. (2001), found that their predicted trend in troposphere–stratosphere mass exchange was a ramification of more wave activity propagating from the troposphere into the stratosphere. Other models have produced apparently conflicting planetary wave responses to climate change (Austin et al. 2003). For instance, Shindell et al. (2001) and Pitari et al. (2002) both report a reduction in the propagation of planetary waves in high northern latitudes, while Gillett et al. (2002) and Sigmond et al. (2004) predict a future increase in overall generation of planetary waves. Because of these differing planetary wave responses, it has not been possible to obtain a consensus as to what will happen to the Brewer–Dobson circulation in a changing climate.

Part of the difficulty is the different ways the planetary waves are analyzed in each of the published studies. Here we make a systematic assessment of how climate change will affect the Brewer–Dobson circulation by comparing the same diagnostics from 13 climate change experiments performed with ten models. All the models had an upper boundary above the stratopause and hence include the entire stratosphere in their domain. Both transient and equilibrium experiments are considered, as well as models with and without chemistry (see Sect. 2 for details). Following Butchart and Scaife (2001) we compare the mass exchange across the tropical tropopause in the 13 experiments (Sect. 3). To assess how planetary wave driving responds to the climate change in these experiments we derive in Sect. 4 the extra-tropical stratosphere-to-troposphere mass fluxes from the Eliassen and Palm (EP) flux divergence using the Cambridge downward control principle (Haynes et al. 1991). Discussion and concluding remarks are given in Sect. 5.

2 Models and experiments

Results were obtained from 11 groups participating in the GCM Reality Intercomparison Project for SPARC (GRIPS; Pawson et al. 2000) who had, also, performed climate change experiments with increased well mixed greenhouse gas (WMGHG) concentrations. As all the models were used for the GRIPS, the upper boundaries were at or above the stratopause but, otherwise, the models had a wide range of horizontal and vertical resolutions (see Table 1 and experiment descriptions below). The models also had quite different representations of the momentum deposition in the middle atmosphere from sub-grid scale waves. For instance, while all but two of the models included a parametrization for orographic gravity wave dissipation only five included a parametrization for non-stationary gravity waves. The other models had a more rudimentary approach based on Rayleigh friction.

This study was based on existing simulations so there was no overall constraint to have identical external forcings or sea surface temperatures (SSTs) in the different models. The comparison includes both transient and equilibrium experiments. In the transient experiments the WMGHG concentrations increased according to either the IS92a scenario or the SRES-A2 scenario (IPCC 2001), though some of the runs also included past changes. The equilibrium experiments establish the change either between particular decades (e.g., 1960s and 1990s) or for a fixed increase in equivalent CO_2 amounts (e.g., $2 \times CO_2$). Some of the models also include coupled ozone chemistry and hence include the effects of ozone changes, too. In a few cases, experiments were available from the same GCM with and without coupled chemistry, enabling the effects of chemical feedbacks to be considered. Brief descriptions of the individual experiments are given below, with the key points of the model formulations summarized in Table 1.

Table 1 Model details

Model	No. of levels	Upper boundary (hPa)	Resolution		Parametrized drag		
			Horizontal	Vertical	O	NO	RF
CMAM	50	0.000637	T32 (48 × 96)	2.0–3.0	√	√	
FUB-CMAM	34	0.0068	T21 (32 × 64)	2.0–3.5			√
GISS(chem)	23	0.002	24 × 36	4.0–5.0	√	√	
IGCM	26	0.1	T21 (32 × 64)	2.3			√
MAECHAM4chem	39	0.01	T42 (64 × 128)	1.5–2.0	√	√	
MRI	30	0.4	T42 (64 × 128)	2.0	√		√
UM49L	49	0.1	72 × 96	1.4	√		√
UM64L(chem)	64	0.01	72 × 96	1.3	√	√	
UM64LS	64	0.01	72 × 96	1.3	√		√
WACCM	66	5.1×10^{-6}	T63 (64 × 128)	1.5–2.0	√	√	

For grid point models the horizontal resolution is given as no. of latitude grid points × no. of longitudinal grid points. For spectral models both the spectral truncation and equivalent grid point resolution are given. The vertical resolution is the vertical grid spacing in km in the stratosphere. In many of the models this is much finer near the tropopause and gradually becomes coarser toward the upper boundary, therefore a range of resolutions is given. The final three columns indicate how sub-grid scale processes are parametrized in the zonal momentum equation in the middle atmosphere

O orographic scheme, *NO* non-orographic, or spectral scheme, *RF* Rayleigh friction

2.1 CMAM

Two 20-year equilibrium runs were performed with the Canadian Middle Atmosphere Model (CMAM; de Grandpré et al. 2000) representative of the current and $2 \times CO_2$ conditions. These simulations used a prescribed ozone climatology, and the momentum depositions by a broad spectrum of sub-grid scale gravity waves and orographic gravity waves were parametrized according to Medvedev and Klaassen (1995) and McFarlane (1987), respectively. The control simulation used WMGHG concentrations specified from observations as of 1987 and prescribed SSTs and sea-ice distributions from Shea et al. (1990). For the perturbed scenario, the CO_2 mixing ratio was set to 696 ppmv and the SSTs and sea-ice distributions altered according to the anomalies predicted from a transient simulation with the CCCma coupled climate model (Boer et al. 2000).

2.2 FUB-CMAM

Three 20-year time-slice simulations were performed with the Freie Universität Berlin Climate Middle Atmosphere Model (FUB-CMAM; Pawson et al. 1998; Langematz 2000). The model includes vertical diffusion and Rayleigh friction in the mesosphere. Monthly mean SSTs including an annual cycle but no interannual variability were prescribed, as well as the ozone and CO_2 distributions. A ''1980'' simulation used a zonal mean ozone climatology based on measurements for 1978–1983 and a CO_2 concentration of 300 ppmv; a ''2000'' simulation took into account the observed stratospheric ozone depletion; and a second ''2000'' simulation took into account the observed stratospheric ozone change plus the 11% increase in the amount of CO_2 from 1980 to 2000 (Langematz et al. 2003).

2.3 GISS/GISSchem

Results were obtained from two 110-year experiments using the NASA Goddard Institute for Space Studies (GISS) model II in which the concentrations of WMGHG were prescribed according to observations from 1959 to 1985 and subsequently followed the IPCC IS92a scenario from 1986 to 2069 (Shindell et al. 2001). A gravity wave parametrization including generation from orography, wind shear and convection was used. Both runs were performed using a mixed-layer ocean. In one experiment (''GISS''), climatological ozone was used while the other (''GISSchem'') included parametrized stratospheric chemical response to climate conditions and halogen abundances (Shindell and Grewe 2002). Halogen trends are similar to those in WMO (1999). In all other respects, aside from slightly different initial conditions, the two runs were identical.

2.4 IGCM

The Intermediate General Circulation Model (IGCM) developed at Reading University is a model of intermediate complexity (see Forster et al. 2000; Taylor and Bourqui 2005 for a description). The version used here includes an updated version of the Morcrette (1991) radiation scheme in both short and long waves. Rayleigh friction is applied in the top five levels. Surface temperatures are specified from a time-varying

climatology. Results were obtained from three 20-year time-slice simulations: a control simulation for 1979 conditions, a 1997 simulation with only the CO_2 concentration increased, and a 1997 simulation with the concentrations of all the WMGHGs increased. Ozone was specified from a three-dimensional monthly varying climatology averaged over 1985–1989 from Li and Shine (1995). CO_2, CH_4, N_2O, CFC-11 and CFC-12 are specified with constant mixing ratios calculated according to IPCC (2001).

2.5 MAECHAM4chem

The MAECHAM4chem GCM included parametrizations of both orographic and non-stationary gravity waves (Manzini et al. 1997; Manzini and McFarlane 1998) and interactively coupled stratospheric chemistry (Steil et al. 2003). Results were obtained from three 20-year simulations with GHG concentrations representative of the 1960s, 1990s and 2000 (Manzini et al. 2003; Steil et al. 2003) and a fourth 20-year simulation with GHG concentrations for 2030 from the WMO (1999) scenarios. All the simulations use 20-year averaged climatological SSTs for the respective conditions, either from observations or from scenarios simulations performed with the low top ECHAM4 model (Roeckner et al. 1996).

2.6 MRI

The MRI model (Yukimoto et al. 2001; Shibata et al. 1999) includes a parametrization of orographic gravity wave drag and Rayleigh friction in the middle atmosphere. The atmosphere component is coupled to a 23 level global ocean model with a latitude-longitude resolution varying from $2° \times 2.5°$ poleward of 12° to 0.5° at the equator. Results are available from 41 years of simulation in which the GHGs followed the SRES-A2 scenario from 2040 to 2080, and a 30 year control simulation for 1990s conditions. Climatological ozone was used.

2.7 UM49L

The 49 level version of the Met Office Unified Model (UM) had orographic gravity wave-drag parametrized up to 20 hPa and Rayleigh friction applied in the mesosphere (see Butchart et al. 2000 for details). Results were obtained from two 60-year runs [Runs (a) and (b) of Butchart et al. (2000)] in which the concentrations of WMGHG were prescribed according to the IPCC IS92A scenario for 1992–2051. Climatological ozone was used and sea surface conditions were taken from a separate coupled ocean–atmosphere model experiment using the same WMGHG scenario. The two runs were identical apart from the initial conditions which nonetheless were both representative of the early 1990s. So as not to give undue weight to this model only results from run (b) are used in this study. Butchart and Scaife (2001) showed that both runs gave similar results when diagnosing upwelling.

2.8 UM64L/UM64Lchem

The 64 level version of the UM is similar to UM49L but with raised upper boundary and the Rayleigh friction replaced by the Warner and McIntyre (1999) Ultra Simple Spectral Parametrization (USSP) of gravity waves as described in Scaife et al. (2002). Improvements were also made to some of the other physical parametrizations (Scaife et al. 2002). Results were obtained from two 40-year experiments with (''UM64Lchem''; Austin and Butchart 2003) and without (''UM64L''; Hare et al. 2005) the ''UMETRAC'' coupled stratospheric chemistry (see Austin and Butchart 2003 for details of the UMETRAC chemistry). In both simulations the SSTs and sea ice were specified from observations (1980–1999), or using the trends (but keeping the observed variability) from a coupled ocean–atmosphere version of the model (2000–2019). WMGHG concentrations were specified according to the IPCC scenario IS92a. In the coupled chemistry run the halogen amounts were specified according to WMO (1999).

2.9 UM64LS

This version of the UM differs from UM64L in two respects. First it has Rayleigh friction instead of the spectral gravity wave scheme. Secondly it uses a thermodynamic, or slab ocean, thus allowing the SSTs to evolve in response to the changing forcing. The thermodynamic ocean has no explicit heat transports, rather these are diagnosed during any initial calibration phase, and then held constant. Results were obtained from equilibrium runs with preindustrial CO_2 abundance, double preindustrial CO_2 abundance and quadruple preindustrial CO_2 abundance (see Gillett et al. 2003 for details).

2.10 WACCM

The Whole Atmosphere Community Climate Model version 1b (WACCM), is based on the National Center for Atmospheric Research (NCAR) Community Climate Model version 3, CCM3 (Kiehl et al. 1998;

Williamson 1997). In addition to the parametrizations used in CCM3, WACCM includes parametrizations for the upper atmosphere. These include: a spectrum of non-orographic waves, molecular diffusion, non-LTE cooling due to CO_2 and a simplified parametrization of ion drag (Sassi et al. 2002, 2004). Results were obtained from a 22-year simulation using observed SSTs and GHG concentrations for the period 1979–2000.

3 Tropical upwelling

3.1 Annual mean climatology

Because the Brewer–Dobson circulation describes Lagrangian-mean transport it can not be diagnosed directly from the Eulerian velocity fields in the models. Instead we use the transformed Eulerian mean residual velocities ($\overline{v^*}, \overline{w^*}$) (Andrews and McIntyre 1976, 1978) which approximate the mean meridional mass transport for seasonally averaged conditions (e.g., Holton 1990). Figure 1 shows the annual mean $\overline{w^*}$ from each model for 1990 conditions (see figure legend for details). All the models have upwelling throughout the tropical stratosphere and downwelling in the extra-tropics, characteristic of the classical Brewer–Dobson overturning circulation. The upwelling regions extend roughly 30° either side the equator, though there are variations in width of about 10° between the models.

In the lower stratosphere the strength of the Brewer–Dobson circulation is directly related to the amount of tropical upwelling and hence the mass flux from the troposphere. At ~ 70 hPa the annual mean $\overline{w^*}$ in the tropics peaks at about 0.3 mm s^{-1} in the models (Fig. 2) and when averaged from 20° S to 20° N the multi-model mean $\overline{w^*}$ is 0.25±.015 mm s^{-1} which is the same as that which can be derived from the 10-year (1992–2001) mean of UK Met Office stratospheric analyses (Swinbank and O'Neill 1994). The residual vertical velocities are, however, not uniform across the tropics and many of the models have a local minimum near the equator with maxima 15–20° either side (see Fig. 1). This feature can also be seen in the Met Office analyses (Fig. 2).

3.2 Seasonal cycle

Figure 3 shows that a local minimum in the upwelling near the equator is present in all seasons in all the models apart from GISS, GISSchem and UM49L. In most models the maximum upwelling is in the summer sub-tropics, consistent with the findings of Plumb and Eluszkiewicz (1999) and Rosenlof (1995), and the upwelling region is displaced 10–20° toward the summer pole, explaining the double peak in the annual mean in Fig. 2. The only runs not to reproduce this feature are GISS and GISSchem and in these runs the maximum upwelling is pushed toward the equator in the boreal summer. Possibly this is because, with the coarse vertical resolution around the tropopause, the GISS results are affected by the top of the Hadley cell. In general, inter-model differences are quite large, except between the same model with and without ozone chemistry (cf. GISS and GISSchem, or UM64L and UM64Lchem in Fig. 3).

An important consequence of the seasonal movement of the upwelling region into the summer hemisphere is that mass fluxes calculated from the annual mean residual vertical velocities (e.g., Figs. 1, 2) are underestimated. Therefore in this study we use annual mean mass fluxes based on the average of the net upward mass flux in each season. Figure 4 shows the seasonal anomalies from this annual mean mass flux at ~ 70 hPa. In most of the models there was a strong annual cycle with the largest fluxes in December–January–February (DJF) due to more planetary waves propagating and breaking in the boreal winter stratosphere than in the austral winter. In these models the mass fluxes in DJF were often 50% larger than those in June–July–August (JJA). In a few of the models (GISS, GISSchem MAECHAM4chem) the seasonal cycle was more semi-annual than annual (again see Fig. 4), mainly because of a weak annual component rather than an exceptionally strong semi-annual component. These models had downwelling in the northern subtropics with a second region of upwelling further north. In the IGCM the seasonal cycle is reversed, mainly due to the large upward residual circulation which occurs in the simulations during the summer time in the northern hemisphere sub-tropics near the tropopause (see Fig. 3). Note that this anomalous circulation is local and is not present anymore at levels higher than 50 hPa.

In general, the amplitude of the seasonal cycle is much larger than the inter-annual variability in the mass fluxes (cf. Fig. 4 and upper panel in Fig. 5). The greatest variability is, however, between the models. Figure 5 shows that, for similar GHG loadings, the mass fluxes could still be up to 50% different, despite the similarities in the residual vertical velocities (cf. Fig. 2). It is not clear what causes this inter-model variability and there is no obvious connection to model resolution. Once again, the results for GISS and GISSchem are very similar in Fig. 5 but the difference between UM64L and UM64Lchem are larger than the inter-annual variability in the runs. Hence in that

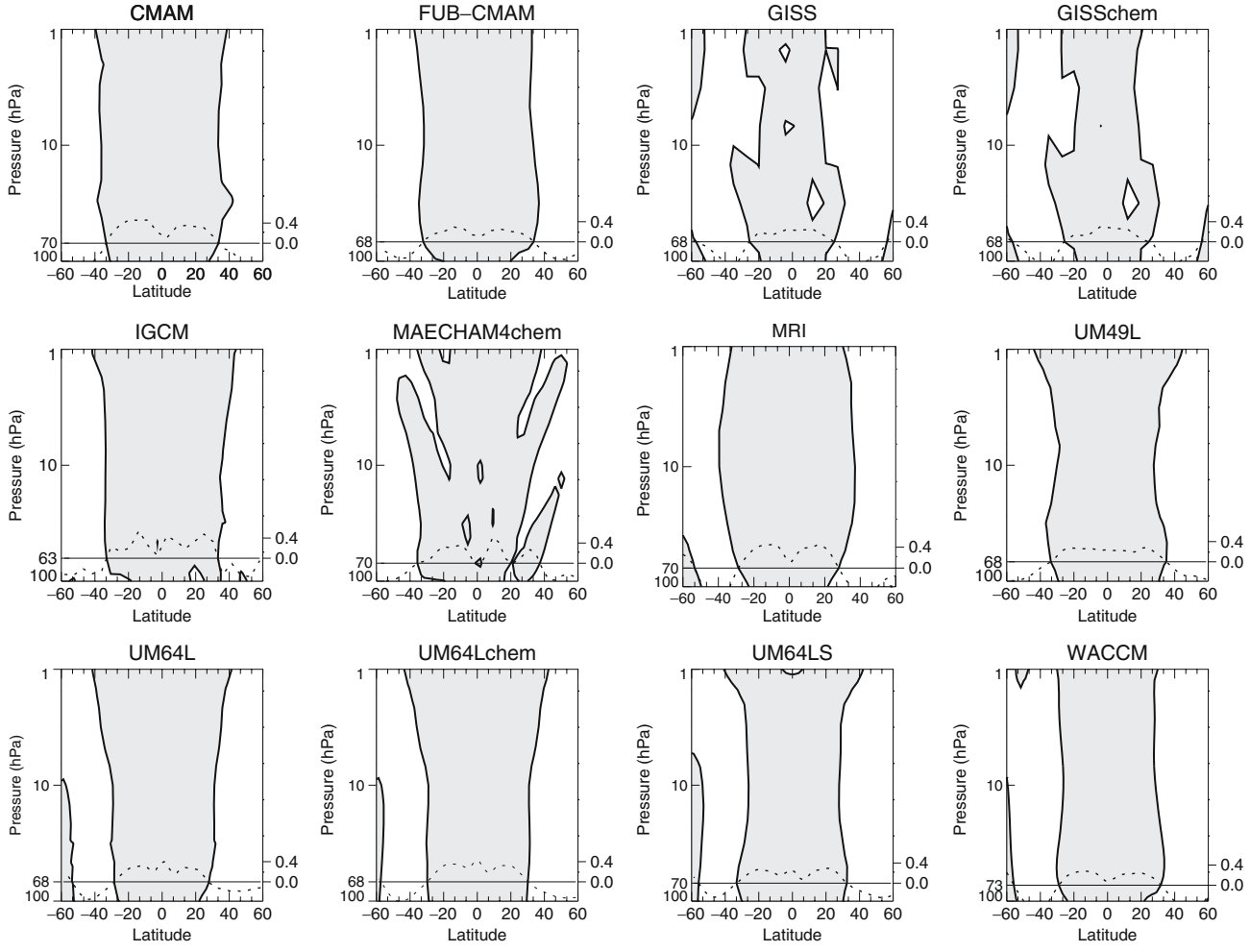

Fig. 1 Meridional cross-sections of the annual mean residual vertical velocities for each model. Climatological means are shown for the 1990s. For the equilibrium experiments results were taken from the run closest to 1990 conditions, i.e. the $1 \times CO_2$ run for CMAM, the "2000" run for FUB-CMAM including both GHG and O_3 changes, the "1997" run of the IGCM with all GHG changes, the "2000" run of MAECHAM4chem, the control run for MRI, and $1 \times CO_2$ run for UM64LS. For the transient runs (GISS, GISSchem, UM49L, UM64L, UM64Lchem and WACCM) the 10-year mean for 1991–2000 (1992–2001 for UM49L) is shown. Only the zero contour is shown and upwelling regions are *shaded*. The *dotted curves* indicate the strength (right hand ordinate) of the upwelling velocities in mm s^{-1} at ~ 70 hPa (see *horizontal line* for precise level for each model)

model the mean circulation strength appears to be affected by the inclusion of ozone chemistry, though this is probably more due to systematic differences between the prescribed and predicted ozone climatologies used in the two runs than the coupling per se.

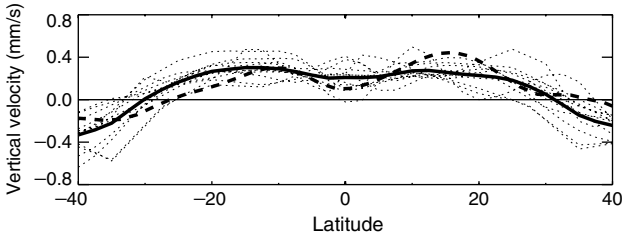

Fig. 2 *Dotted lines* annual mean residual vertical velocities at ~ 70 hPa as in Fig. 1. The *thick line* is the multi-model mean and the *thick dashed line* is the 10-year mean (1992–2001) from the UK Met Office analyzes at 68 hPa

3.3 Trends

In response to the rise in WMGHG concentrations, all the experiments predicted an increase in the annual mean mass flux entering the stratosphere (Fig. 5), equivalent to a trend of about 2% per decade. This was due to a strengthening of the Brewer–Dobson circulations in the experiments, with the width of the tropical upwelling regions remaining largely unaffected by climate change (not shown). Eventually, the increase in mass flux may, however, saturate as the increase in mass flux in the UM64LS from 2 to 4 × CO_2 is smaller

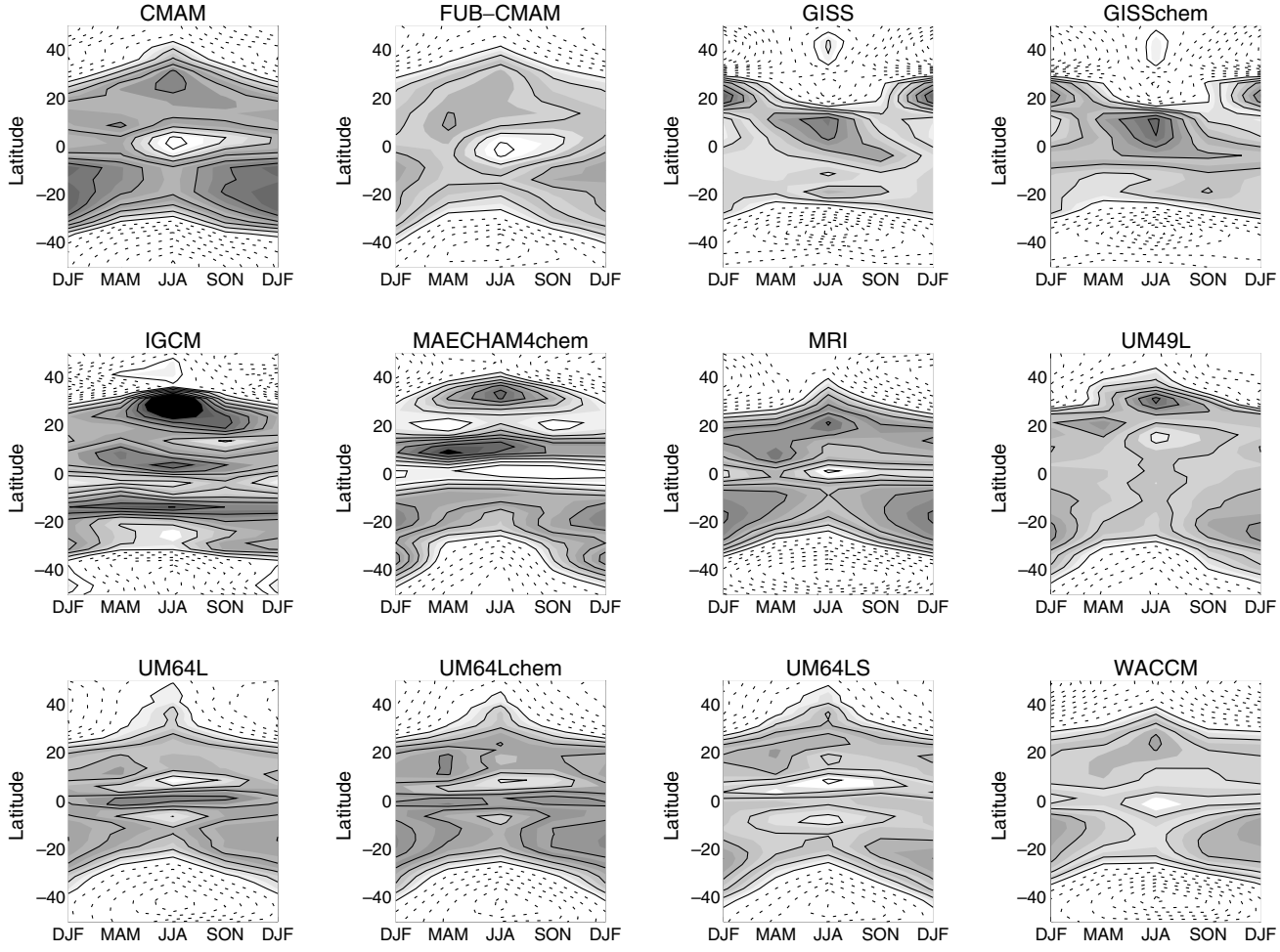

Fig. 3 Seasonal and latitudinal variations in the residual vertical velocities in the lower stratosphere for 1990 conditions as defined in Fig. 1. See *horizontal lines* in the respective panels in Fig. 1 for the precise levels. The contour interval is 0.1 mm s^{-1} and *shading* denotes upwelling with the darker shading corresponding to stronger upwelling

than the increase from 1 to 2 × CO_2 in Fig. 5. Some studies have found similar sensitivity for other climate variables due to a saturation of the CO_2 radiation absorption bands though for the simulations used here there was no evidence of a change in the climate sensitivity of the global mean temperature from 2 to 4 × CO_2. The two ''1997'' IGCM runs and the two ''2000'' FUB-CMAM runs can not be distinguished in Fig. 5, though the difference for the IGCM runs can be seen in Fig. 6a which summarises the trend from all the climate change experiments.

The multi-model average trend (Fig. 6) in the annual mean mass flux is 11.0 ± 2.0 kt s^{-1} $year^{-1}$, though there is considerable spread between models (Fig. 6a). Models with the smallest trends are those simulating past changes (FUB-CMAM, IGCM, WACCM). Models simulating both past and future changes (GISS, GISSchem, MAECHAM4chem, UM64L, but not UM64Lchem) also had smaller trends over the period when observed SSTs were used, than over the full period of the integration. The reason for the smaller trends in the past are unclear. It has been argued that the declining stratospheric ozone in the latter part of the twentieth century reduces wave activity propagating into stratosphere and thereby weakens the Brewer–Dobson circulation (Hu and Tung 2003). However, the effects of ozone changes are not included in many of the experiments reported here (e.g., IGCM, UM64L, WACCM) and the only significant difference between the past and future simulations is the switch from observed to model predicted SSTs. Also, results from FUB-CMAM with observed ozone changes from 1980 to 2000, but no GHG changes, showed a positive trend in annual mean mass exchange rate of 1.2 kt s^{-1} $year^{-1}$.

As noted by Butchart and Scaife (2001) the increase in mass flux generally occurs throughout the year, though Figs. 6b and c show that, for most of the models, the trend is larger in DJF than in JJA.

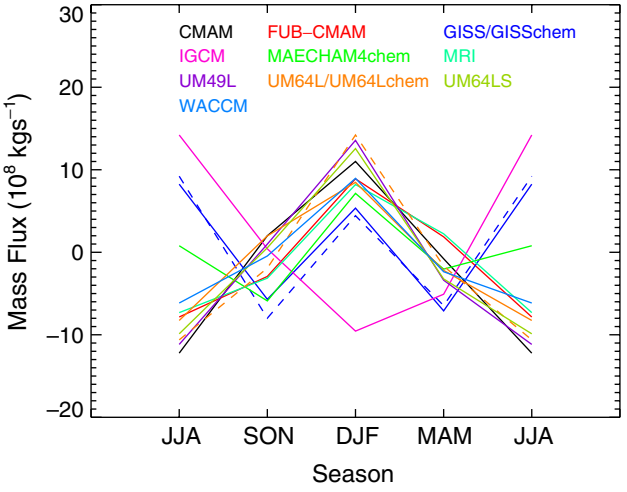

Fig. 4 Seasonal cycle in upward mass flux in the lower stratosphere derived by multiplying the residual vertical velocities in Fig. 3 by a scaling proportional to the cosine of latitude to convert to a mass flux and integrating over all latitudes in Fig. 3 where $\overline{w^*}$ is positive. Seasonal anomalies from the annual mean are plotted. Where there are results from the same model with and without chemistry the results are shown in the *same colour* with the *dashed curve* representing the run with chemistry

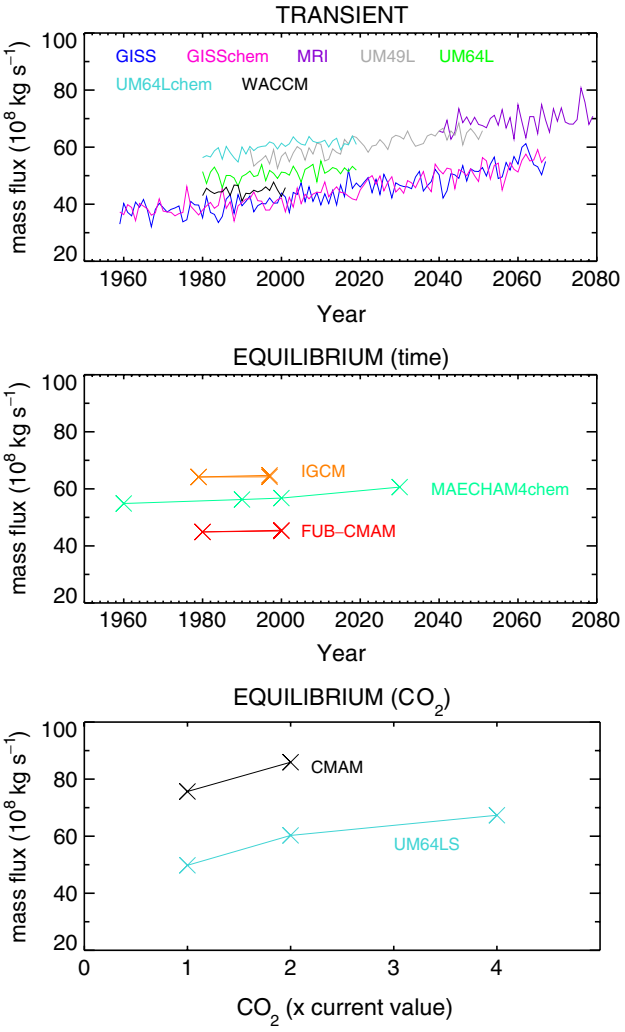

Fig. 5 Annual mean upward mass flux in the tropical lower stratosphere for each model at the levels indicated in Fig. 1. A time sequence is shown for the transient experiments (*top panel*) and the multi-annual mean for the equilibrium runs (*lower two panels*)

However, because of the generally larger fluxes in DJF than in JJA (see Fig. 4), the proportional changes in percent per year (not shown) are similar in the two seasons. On the other hand, the larger mass flux trend in DJF implies the residual vertical velocities at the tropical tropopause will increase more during the northern hemisphere winter than summer, which can only serve to enhance the annual cycle in the tropical tropopause temperatures. Again, in both DJF and JJA, the simulated trends for the past (FUB-CMAM, IGCM and WACCM) are the smallest. FUB-CMAM was unusual in having a significant downward trend in JJA, possibly due to specified ozone changes, particularly a reduction over Antarctica. Overall there is a greater spread in trends in DJF probably because the larger variability of the northern hemisphere planetary waves in winter makes them more sensitive to model formulation than in the southern hemisphere.

4 Wave driving

4.1 Downward control

For steady conditions the Cambridge downward control principle (Haynes et al. 1991) gives the meridional mass streamfunction $\Psi(\phi, z)$ at latitude ϕ and log(pressure)-height, z, in terms of the vertical integral of the eddy induced zonal forces, $\mathscr{F}$, above z, i.e.

$$\Psi(\phi, z) = \int_z^\infty \left\{ \frac{\rho_0 a^2 \mathscr{F} \cos^2\phi}{\partial \bar{m}/\partial \phi} \right\}_{\bar{m}=\text{const.}} \mathrm{d}z',$$

where a is the Earth's radius and ρ_0 a basic state density. The integration is up a line of constant zonal mean absolute angular momentum $\bar{m} = \overline{m(z,\phi)}$ (Haynes et al. 1991), though as these are nearly vertical, except near the equator, we approximate the calculation in this study by integrating at constant latitude. In the model simulations there are contributions to $\mathscr{F}$ from the resolved waves, given by the EP-flux divergence (Andrews and McIntyre 1976, 1978), and from the sub-grid scale waves, represented by the parametrized gravity wave drags and, for those

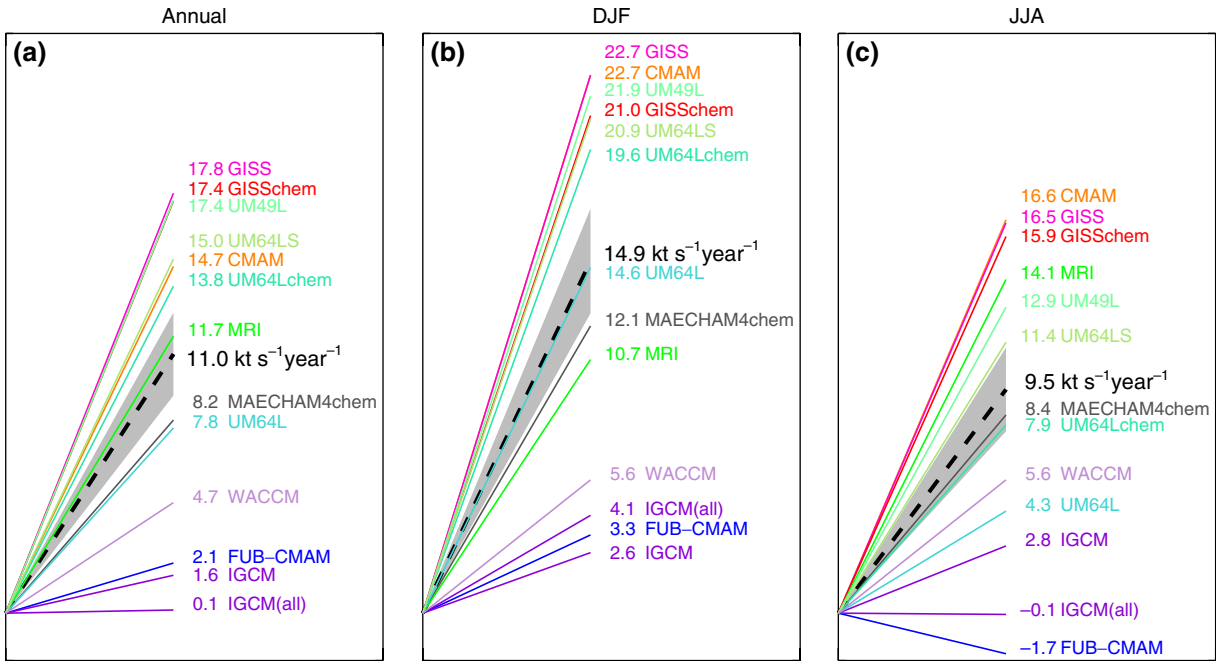

Fig. 6 Schematic representation of the trends in the upward mass flux in the tropical lower stratosphere for each model at the levels indicated in Fig. 1, in kt s^{-1} $year^{-1}$: **a** annual mean, **b** DJF mean, and **c** JJA mean. For the transient experiments, and also for the four MAECHAM4chem runs, trends are based on a least squares linear fit. The trend for the UM64LS is calculated from the difference between $1 \times CO_2$ and $2 \times CO_2$ runs. As with the CMAM experiment it is assumed that doubling of CO_2 took place over 70 years. The *dashed line* is the multi-model mean with the standard error given by the *grey shading*. So as not to give undue weight to the IGCM, the two trends from this model were averaged and treated as single trend when calculating the multi-model mean

models which include it, a contribution from the Rayleigh friction. Other numerical processes, such as numerical truncation and diffusion, can contribute but these are small apart from, perhaps, near the upper boundaries. Nonetheless, given the density weighting of the downward control integrand, it is unlikely that there will be any direct upper boundary effects on the streamfunction calculated for the lower stratosphere, especially as the upper boundaries are at or above the stratopause in accordance with the requirements of the GRIPS (Pawson et al. 2000).

The mass streamfunction Ψ is defined such that the transformed-Eulerian-mean residual mean velocities, $(\overline{v^*}, \overline{w^*})$, are given by

$$\overline{v^*} = -\frac{1}{\rho_0 a \cos\phi}\frac{\partial \Psi}{\partial z}, \quad \overline{w^*} = \frac{1}{\rho_0 a \cos\phi}\frac{\partial \Psi}{\partial \phi}$$

This implies $\overline{w^*} = 0$ at $\Psi_{\max}$ and $\Psi_{\min}$ and therefore in the lower stratosphere the maximum and minimum of Ψ determine the latitudes at which the tropical upwelling changes to extra-tropical downwelling—the so-called turnaround latitudes (Rosenlof 1995). Poleward of latitude ϕ the net downward mass flux is then given by

$$2\pi \int_{\phi}^{\text{pole}} \rho_0 \cos\phi \overline{w^*} a \mathrm{d}\phi = 2\pi a \Psi(\phi),$$

with the boundary condition $\Psi = 0$ at the poles (e.g., see Rosenlof 1995). Consequently it follows that the extra-tropical downwelling mass flux which balances the upwelling mass flux in the tropics is given by

$$2\pi a(\Psi_{\max} - \Psi_{\min}).$$

4.2 Streamfunctions

Figure 7 compares for each model at ~ 70 hPa the annual mean streamfunction derived from the EP-flux divergence using the downward control principle (black curve) with streamfunctions derived directly from the residual vertical velocities (grey curve). For each model the curves are representative of 1990s conditions (see figure legend for details) and thickness is an indication of the interannual variability (again see figure legend for details). Interannual variability is not shown for the IGCM, MAECHAM4chem and

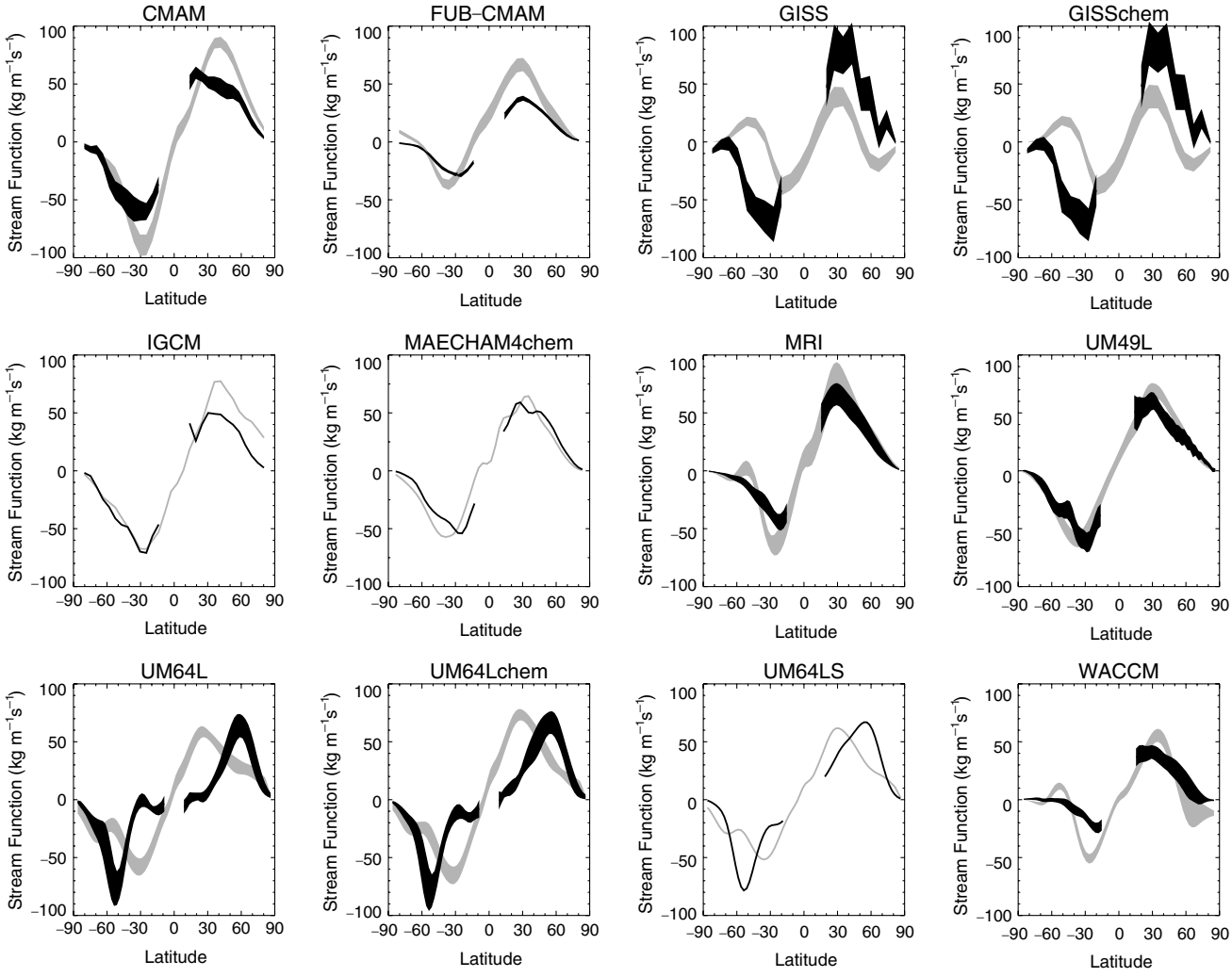

Fig. 7 Annual mean mass streamfunctions (kg m^{-1} s^{-1}) at ~ 70 hPa (see *horizontal line* in the respective panels in Fig. 1 for the precise level). *Black curves* as derived from the EP-flux divergence using the downward control principle. *Grey curves* as derived directly from the residual vertical velocities. For each model year the annual mean was calculated from the four seasonal means. For the equilibrium experiments the results shown are for the run closest to 1990 conditions as described in Fig. 1. For CMAM and FUB-CMAM the thickness of the curve denotes the 2 σ deviation either side of the climatological mean. For the transient runs the thickness of the curves again denotes a 2 σ interannual deviation either side of a linear least squares fit to the time series of annual means, with the mean position the linear fit value for 1995. For the IGCM, MAECHAM4chem and UM64LS only multi-year results were available and consequently the stream functions for these models were estimated from the climatological mean data, though data was available for each season

UM64LS equilibrium experiments as only multi-year mean results were available.

For all the models there is reasonably good agreement between the streamfunctions derived from the EP-Flux divergence using downward control and the actual streamfunctions, though the differences are generally much greater than the interannual variations (Fig. 7). Inter-model differences are also quite large compared to the interannual variability of an individual model. Nonetheless, with exception of the 64-level versions of the UM (UM64L, UM64Lchem, and UM64LS), the two streamfunctions for each model indicate almost the same turnaround latitudes (i.e., the latitudes of the maxima and minima). Furthermore these do not change significantly in any of the models in response to increasing concentrations of WMGHGs (results not shown). For the 64 level versions of the UM it is unclear why the turnaround latitudes derived using downward control should be displaced poleward though contributions to the downward control integrand from sub-grid scale momentum deposition in the stratosphere and mesosphere can almost certainly be ruled out because UM64LS uses Rayleigh friction while UM64L has parametrized non-orographic gravity

waves; yet both these models show the same discrepancy between the downward control and modelled turnaround latitudes.

Results from GISS/GISSchem, and UM64L/UM64Lchem, suggest that for this diagnostic the inclusion of interactive ozone chemistry again has little impact.

4.3 Downward control mass fluxes and trends

Apart from the two GISS models and UM64L Fig. 8 shows that the wave-driven extra-tropical stratosphere-to-troposphere mass flux derived from the EP-divergence (black curves and symbols) provides 60% or more of the flux required to balance the tropical upwelling (grey curves and symbols). The contribution is generally smallest in those models with coarser horizontal resolution (e.g. CMAM, FUB-CMAM, IGCM), presumably, because these models do not represent as much of the spectrum of waves, though the contributions in the southern hemisphere in the WACCM are also relatively small. The exceptions to this rule are the GISS and GISSchem simulations for which the mass fluxes calculated from downward control significantly over estimate that required to balance the tropical upwelling fluxes (see Fig. 8). In this case this is probably due to the rather poor vertical resolution (5 km) throughout the stratosphere which

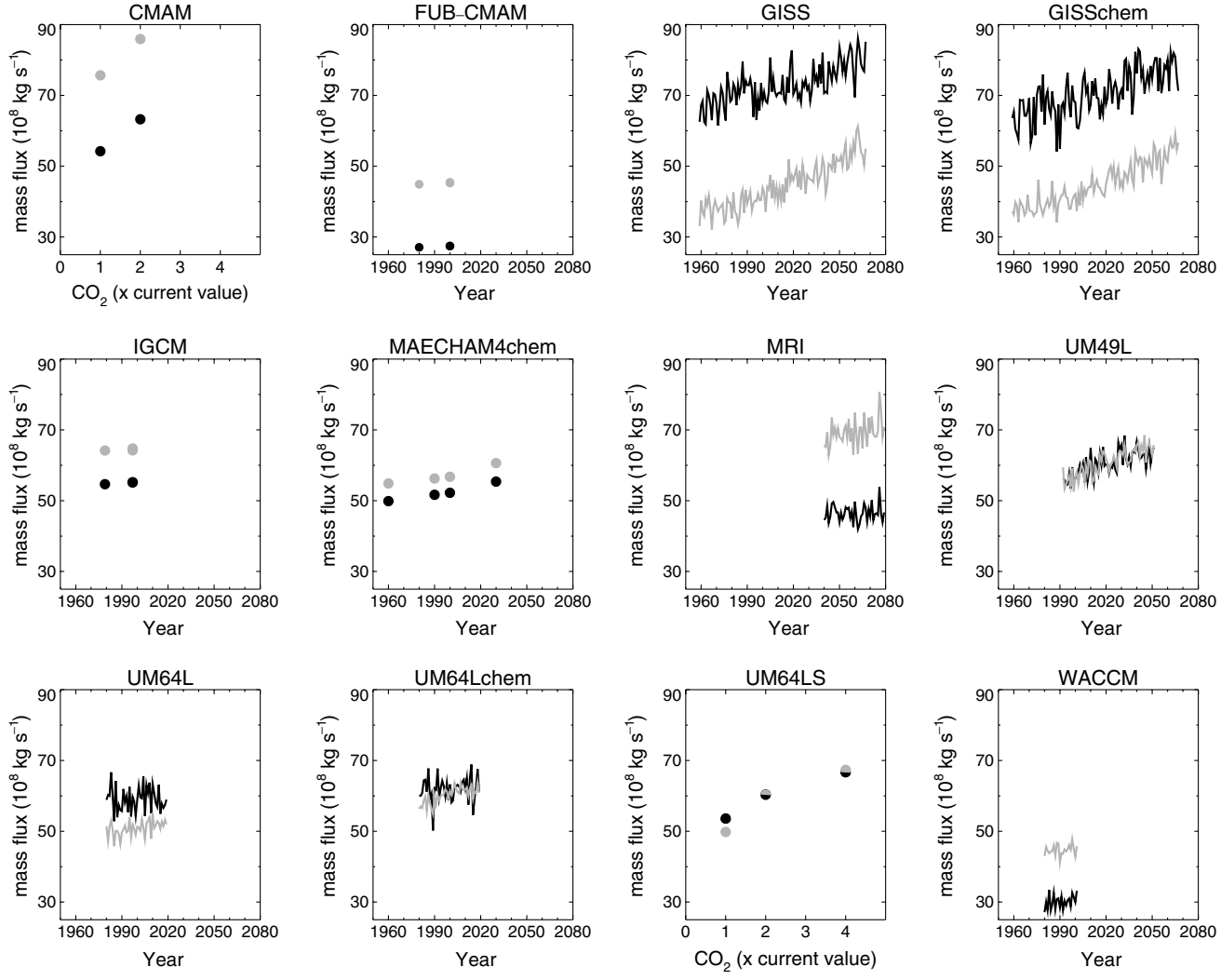

Fig. 8 *Black curves and symbols* annual mean extra-tropical downwelling mass flux at ~ 70 hPa (see *horizontal line* in the respective panels in Fig. 1 for the precise level) derived from the EP-flux divergence by applying the downward control principle. *Grey curves and symbols* annual mean tropical upwelling mass flux derived directly from the residual vertical velocities (see Fig. 5). A time sequence is shown for the transient experiments (GISS, GISSchem, MRI, UM49L, UM64L, UM64Lchem, and WACCM) and the multi-annual mean for the equilibrium experiments (CMAM, FUB-CMAM, IGCM, MAECHAM4chem, UM64LS)

means the vertical contribution to the EP-flux divergence and, in particular, its vertical position may not be well represented and this can have a big effect on the downward control integral.

As well as being able to balance over 60% of the tropical upwelling, the changes in the downward control mass fluxes due to increasing concentrations of WMGHGs are consistent with the concomitant changes in the tropical upwelling (see Fig. 8). Further evidence that the amount of tropical upwelling responses to changes in the wave forcing (EP-flux divergence) is given by the correlation between the inter-annual variations in the tropical upwelling and downward control mass fluxes (Table 2). For the annual mean mass fluxes the average correlation for the 11 simulations in Table 2 is 0.64, though for most models the correlation is higher than this and only the two GISS simulations have correlations below 0.5. Interestingly this would suggest that in this model resolved atmospheric wave driving is not the dominant cause of the inter-annual variability at least for the Brewer–Dobson circulation. This is consistent with the GISS model having the coarsest resolution and therefore naturally resolves the fewest waves. Despite this, the trend in the wave driven mass flux agrees well with the trend in the tropical upwelling for both GISS and GISSchem. The poor correlation in the WACCM simulation in JJA is probably linked to the rather weak non-stationary planetary wave forcing in that model in the southern hemisphere (see above).

Table 2 Correlation at ~ 70 hPa (see Fig. 1 for precise level) between the inter-annual variability in the annual and seasonal mean (DJF and JJA) tropical upwelling mass fluxes derived from the residual vertical velocities and the extra-tropical downwelling mass fluxes derived from the EP-flux divergence assuming downward control

Model	Correlation		
	Annual	DJF	JJA
CMAM ($1 \times CO_2$)	0.77	0.48	0.45
CMAM ($2 \times CO_2$)	0.81	0.50	0.81
FUB-CMAM (“1980”)	0.57	0.64	0.59
FUB-CMAM (“2000”)	0.82	0.80	0.47
GISS	0.36	0.41	0.29
GISSchem	0.37	0.48	0.29
MRI	0.81	0.81	0.62
UM49L	0.68	0.66	0.74
UM64L	0.65	0.56	0.77
UM64Lchem	0.66	0.62	0.67
WACCM	0.53	0.42	0.15

For the transient runs the linear trend was removed prior to calculating the correlation. The FUB-CMAM “2000” simulation is that including both ozone and GHG changes (see Sect. 2). The IGCM, MAECHAM4chem and UM64LS are not included in the table as only multi-annual mean diagnostics were available from these runs

A summary of the trend in the mass fluxes derived from downward control for each model is presented in Fig. 9. This can be compared directly with Fig. 6 which shows the trends in the actual mass fluxes. For the annual mean all but three of the models (FUB-CMAM, UM64L and WACCM) indicate an increase in the downward control derived mass fluxes in response to climate change with the multi-model mean 6.4 ± 1.9 kt s^{-1} $year^{-1}$. Again, there is considerable variability between models, which tend to be clustered in two groups with high or very low trends. As in Fig. 6, those simulations reproducing past changes generally had the smallest trends. Based on the comparison of the multi-model means in Figs. 6 and 9 the trends driven by the changes in EP-flux divergence account for 58% trend in the annual mean upwelling and 74 and 53% for DJF and JJA, respectively.

5 Discussion and conclusions

The primary aim of this study was to reach a consensus on what would happen in a changing climate to the Brewer–Dobson circulation, or at least the large scale troposphere-to-stratosphere mass exchange as determined by the Brewer–Dobson circulation. To achieve this, output was obtained from 13 climate-change experiments from ten GCMs. The only constraints for results to be included in the study were the models had to satisfy the requirements of the GRIPS and, in particular, have a proper representation of the middle atmosphere up to, at least, the stratopause, and the experiments had to include the response to changes in the concentrations of greenhouse gases. Therefore the study included a wide range of both experiments and models. Nonetheless, all the models reproduced the characteristic Brewer–Dobson circulation with upwelling in the tropics and downwelling in the extra-tropics. As with previous studies (Plumb and Eluszkiewicz 1999; Rosenlof 1995) the maximum upwelling is in the summer sub-tropics, though the local minimum that persisted throughout the year near the equator in many of the models is a new finding. In these models the corresponding local maxima in the sub-tropics strengthened during the summer, consistent with the picture of Plumb and Eluszkiewicz (1999) and Rosenlof (1995).

The numerical experiments assessed here unanimously predict that climate change will increase the annual mean troposphere-to-stratosphere mass exchange rate by 11.0 ± 2.0 kt s^{-1} $year^{-1}$ or about 2%

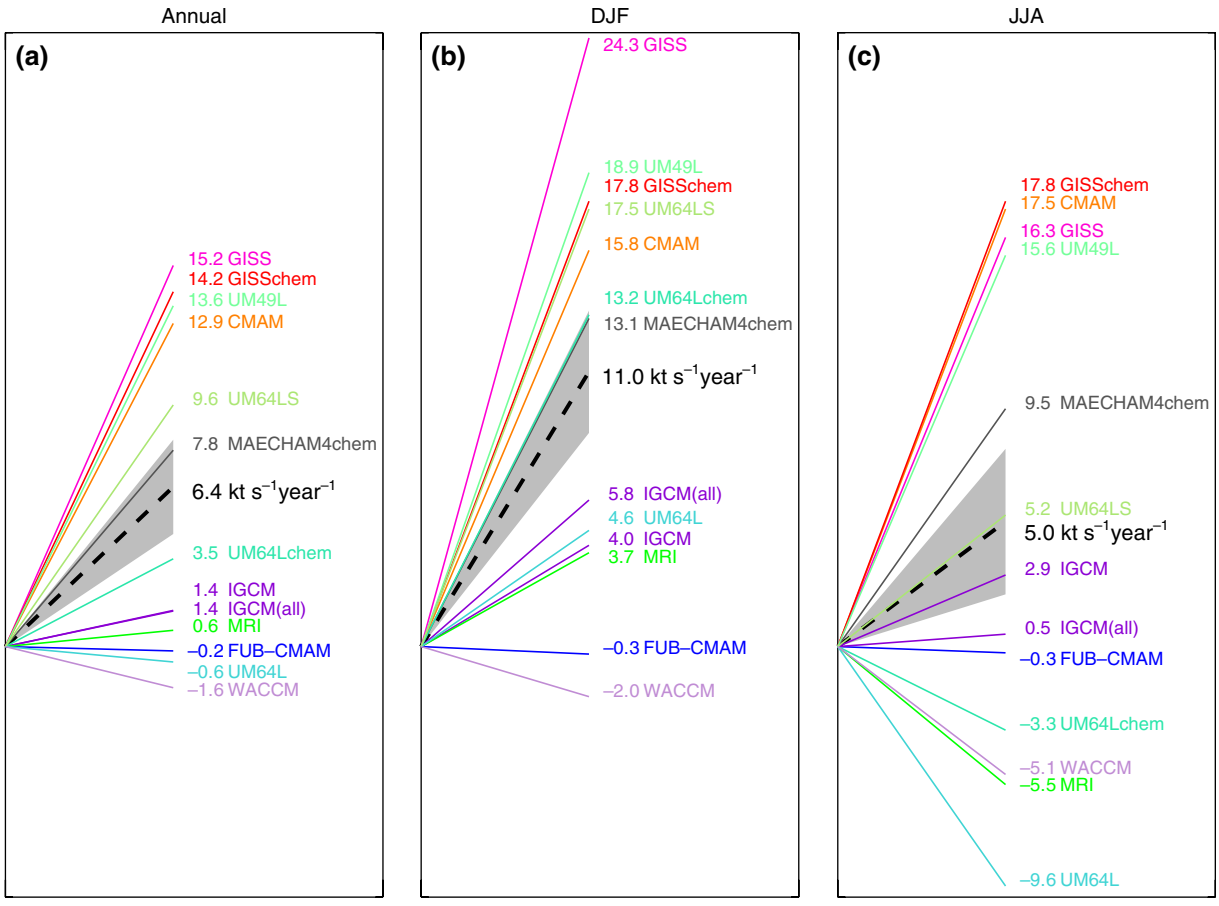

Fig. 9 Schematic representation of the trends in the downwelling mass flux in the extra-tropical lower stratosphere derived from the EP-flux divergence assuming downward control for each model at the levels indicated in Fig. 1, in kt s^{-1} $year^{-1}$: **a** annual mean, **b** DJF mean, and **c** JJA mean. For the transient experiments and also for the four MAECHAM4chem runs trends are based on a least squares linear fit. The trend for the UM64LS is calculated from the difference between $1 \times CO_2$ and $2 \times CO_2$ runs. As with the CMAM experiment it is assumed that doubling of CO_2 took place over 70 years. The *dashed line* is the multi-model mean with the standard error given by the grey shading. So as not to give undue weight the IGCM models, the two trends from this models were averaged and treated as a single trend when calculating the multi-model mean

per decade. Despite considerable inter-model variability a positive trend in the mass exchange rate was a robust feature of all the experiments and, as found by Butchart and Scaife (2001), the trend occurred throughout the year. The multi-model mean trend, however, was larger in DJF than JJA (14.9 and 9.5 kt s^{-1} per year, respectively). Temperature variations in the lower tropical stratosphere are directly related to the residual vertical velocities and a further consequence of the climate change-induced increase in tropical upwelling found in this study is therefore an additional cooling of the lower tropical stratosphere as seen in observations (Thompson and Solomon 2005). The model consensus is for this to be particularly marked in the boreal winter when the models predict the largest increase in the Brewer–Dobson circulation. The seasonal cycle in lower stratospheric tropical temperatures (Yulaeva et al. 1994) is therefore expected to increase with climate change as the boreal winter to spring minimum temperature decreases. It is also interesting to note that the weak seasonal cycle in pollutants such as N_2O that has been detected in observations (Nevison et al. 2004) is thought to be caused by seasonal variations in troposphere–stratosphere mass exchange. The amplitude of this seasonal cycle is therefore also likely to increase as a result of climate change.

In nearly all the models, more than 60% of the tropical upwelling was balanced by extra-tropical downwelling estimated from the wave driving by applying the downward control principle to the EP-flux divergence. In turn, the multi-model mean trend in the downwelling mass fluxes explained 58% of the trend in the tropical upwelling for the annual mean, suggesting that the

strengthening of the Brewer–Dobson circulation in a changing climate results primarily from an increase in resolved wave driving. An important future task is to identify the causes of the increase in wave driving.

Although model resolved driving explains much of the trend, a significant part (~ 40%) cannot be accounted for in the downward control paradigm by changes in the EP-flux divergence alone and, therefore, presumably results from changes in the sub-grid scale momentum deposition in the models. No information on these sub-grid scale processes was collected in this study. In so far as the downward control principle provides an accurate description of the seasonal mean stratospheric behaviour, we conclude that the sub-grid scale processes make a smaller contribution than resolved waves but cannot be neglected when considering the response of the Brewer–Dobson circulation to a changing climate. An important corollary is that the parametrizations of these processes in the models will need to be improved to allow the parameters to respond correctly to climate change.

For this particular study there was little evidence that including interactive ozone would have any significant impact on the conclusions. Finally on the longer timescale there was some evidence from an experiment in which the abundance of CO_2 was quadrupled that the processes driving the trends in the Brewer–Dobson circulation may eventually saturate.

Acknowledgements We would like to thank Kunihiko Kodera and Steven Pawson for agreeing to include this study in the GRIPS as a level 4 task. Discussions with Steven Hardiman, Peter Haynes, and Ted Shepherd were very much appreciated. The IGCM simulations were performed with support by the NERC Upper Troposphere/Lower Stratosphere Thematic Programme (GST022385 and NER/T/S/2002/00058). The UM64L and UM64Lchem simulations were funded by the EU as part of the EuroSPICE project.

References

Andrews DG, McIntyre ME (1976) Planetary waves in horizontal vertical shear: the generalized Eliassen–Palm relation and the mean zonal acceleration. J Atmos Sci 33:2031–2048

Andrews DG, McIntyre ME (1978) Generalized Eliassen–Palm and Charney-Drazin Theorems for waves on axisymmetric mean flows in compressible atmospheres. J Atmos Sci 35:175–185

Austin J, Butchart N (2003) Coupled chemistry-climate model simulations for the period 1980 to 2020: Ozone depletion and the start of ozone recovery. Q J R Meteorol Soc 129:3225–3249

Austin J, Shindell D, Beagley SR, Brühl C, Dameris M, Manzini E, Nagashima T, Newman P, Pawson S, Pitari G, Rozanov E, Schnadt C, Shepherd TG (2003) Uncertainties and assessments of chemistry-climate models of the stratosphere. Atmos Chem Phys 3:1–27

Boer GJ, Flato G, Ramsden D (2000) A transient climate change simulation with greenhouse gas and aerosol forcing: projected climate to the twenty-first century. Clim Dyn 16:427–450

Brewer AW (1949) Evidence for a world circulation provided by measurements of helium and water vapour distribution in the stratosphere. Q J R Meteorol Soc 75:351–363

Butchart N, Scaife AA (2001) Removal of chlorofluorocarbons by increased mass exchange between the stratosphere and troposphere in a changing climate. Nature 410:799–802

Butchart N, Austin J, Knight JR, Scaife AA, Gallani ML (2000) The response of the stratospheric climate to projected changes in the concentrations of well-mixed greenhouse gases from 1992 to 2051. J Clim 13:2142–2159

Dobson GMB (1956) Origin and distribution of the polyatomic molecules in the atmosphere. Proc R Soc Lond 236A:187–193

Forster PM, Blackburn M, Glover R, Shine KP, (2000) An examination of climate sensitivity for idealised climate change experiments in an intermediate general circulation model. Clim Dyn 16:833–849

Gillett NP, Allen MR, Williams KD (2002) The role of stratospheric resolution in simulating the Arctic Oscillation response to greenhouse gases. Geophys Res Lett 29. DOI 10.1029/2001/GL014444

Gillett NP, Allen MR, Williams KD (2003) Modelling the atmospheric response to doubled CO_2 and depleted stratospheric ozone using a stratosphere-resolving coupled GCM. Q J R Meteorol Soc 129:947–966

de Grandpré J, Beagley SR, Fomichev VI, Griffioen E, McConnell JC, Medvedev AS, Shepherd TG (2000) Ozone climatology using interactive chemistry: results from the Canadian Middle Atmosphere Model. J Geophys Res 105(D21):26475–26491

Hare SHE, Gray LJ, Lahoz WA, O'Neill A (2005) On the design of practicable numerical experiments to investigate stratospheric temperature change. Atmos Sci Lett 6:123–127

Haynes PH, Marks CJ, McIntyre ME, Shepherd TG, Shine KP (1991) On the ''downward control'' of the extratropical diabatic circulations by eddy-induced mean zonal forces. J Atmos Sci 48:651–678

Holton JR (1990) On the global exchange of mass between the stratosphere and troposphere. J Atmos Sci 48:392–395

Holton JR, Haynes PH, McIntyre ME, Douglass AR, Rood RB, Pfister L (1995) Stratosphere–troposphere exchange. Rev Geophys 33:403–439

Hu Y, Tung KK (2003) Possible ozone-induced long-term changes in planetary wave activity in late winter. J Clim 16:3027–3038

IPCC (2001) Climate Change 2001: The Scientific Basis. Contribution of Working Group I to the Third Assessment Report of the Intergovernmental Panel on Climate Change. Cambridge University Press, United Kingdom and New York, NY, USA, 881 pp

Kiehl JT, Hack JJ, Bonan GB, Boville BA, Williamson DL, Rasch PJ (1998) The National Center for Atmospheric Research Community Climate Model, CCM3. J Clim 11:1131–1149

Langematz U (2000) An estimate of the impact of observed ozone losses on stratospheric temperature. Geophys Res Lett 27:2077–2080

Langematz U, Kunze M, Krüger K, Labitzke K, Roff GL (2003) Thermal and dynamical changes of the stratosphere since 1979 and their link to ozone and CO_2 changes. J Geophys Res 108(D1):4027. DOI 10.1029/2002JD002069

Li D, Shine KP (1995) A 4-dimensional ozone climatology for UGAMP models. UGAMP (U.K. Universities Global Atmospheric Modelling Programme) Internal Report No. 35, Meteorology Department, Reading University

Manzini E, McFarlane NA (1998) The effect of varying the source spectrum of a gravity wave parameterization in a middle atmosphere general circulation model. J Geophys Res 103:31523–31539

Manzini E, McFarlane NA, McLandress C (1997) Impact of the Doppler spread parameterization on the simulation of the middle atmosphere circulation using the MAECHAM4 general circulation model. J Geophys Res 102:25751–25762

Manzini E, Steil B, Brühl C, Giorgetta MA, Krüger K (2003) A new interactive chemistry-climate model: 2. Sensitivity of the middle atmosphere to ozone depletion and increase in greenhouse gases and implications for recent stratospheric cooling. J Geophys Res 108(D14):4429. DOI 10.1029/2002JD002977

McFarlane NA (1987) The effect of orographically excited gravity wave drag on the general circulation of the lower stratosphere and troposphere. J Atmos Sci 44:1775–1800

Medvedev AS, Klaassen GP (1995) Vertical evolution of gravity wave spectra and the parameterization of associated wave drag. J Geophys Res 100:25841–25853

Morcrette J-J (1991) Radiation and cloud radiative properties in the ECMWF forecasting system. J Geophys Res 96:9121–9132

Nevison CD, Kinnison DE, Weiss RF (2004) Stratospheric influence on the tropospheric seasonal cycles of nitrous oxide and chloroflurocarbons. Geophys Res Lett 31:L20103. DOI 10.1029/2004GL020398

Pawson S, Langematz U, Radek G, Schlese U, Strauch P (1998) The Berlin troposphere–stratosphere–mesosphere GCM: sensitivity to physical parametrizations. Q J R Meteorol Soc 124:1343–1371

Pawson S, Kodera K, Hamilton K, Shepherd TG, Beagley SR, Boville BA, Farrara JD, Fairlie TDA, Kitoh A, Lahoz WA, Langematz U, Manzini E, Rind DH, Scaife AA, Shibata K, Simon P, Swinbank R, Takacs L, Wilson RJ, Al-Saadi JA, Amodei M, Chiba M, Coy L, de Grandpré J, Eckman RS, Fiorino M, Grose WL, Koide H, Koshyk JN, Li D, Lerner J, Mahlman JD, McFarlane NA, Mechoso CR, Molod A, O'Neill A, Pierce RB, Randel WJ, Rood RB, Wu F (2000) The GCM-reality intercomparison project for SPARC (GRIPS): scientific issues and initial results. Bull Am Meteorol Soc 81:781–796

Pitari G, Mancini E, Rizi V, Shindell D (2002) Impact of future climate and emission changes on stratospheric aerosols and ozone. J Atmos Sci 59:414–440

Plumb RA, Eluszkiewicz J (1999) The Brewer–Dobson circulation: dynamics of the tropical upwelling. J Atmos Sci 56:868–890

Rind D, Lerner J, McLinden C (2001) Changes of tracer distributions in the doubled CO_2 climate. J Geophys Res 106(D22):28061–28080

Roeckner E, Arpe K, Bengtsson L, Christoph M, Claussen M, Dümenil L, Esch M, Giorgetta M, Schlese U, Schulzweida U (1996) The atmospheric general circulation model ECHAM4: model description and simulation of present day climate, MPI Rep 218:90 pp. Hamburg, Germany

Rosenlof KH (1995) Seasonal cycle of the residual mean meridional circulation in the stratosphere. J Geophys Res 100:5173–5191

Sassi F, Garcia RR, Boville BA, Liu H (2002) On temperature inversions and the mesospheric surf zone. J Geophys Res 107. DOI 10.1029/2001JD001525

Sassi F, Kinnison D, Boville BA, Garcia RR, Roble R (2004) Effect of El Nino-Southern Oscillation on the dynamical, thermal and chemical structure of the middle atmosphere. J Geophys Res 109. DOI 10.1029/2003JD004434

Scaife AA, Butchart N, Warner CD, Swinbank R (2002) Impact of a spectral gravity wave parameterization on the stratosphere in the Met Office unified model. J Atmos Sci 59:1473–1489

Shea DJ, Trenberth KE, Reynolds RW (1990) A global monthly sea surface temperature climatology. NCAR Technical Note NCAR/TN345+STR, pp 167

Shibata K, Yoshimura H, Ohizumi M, Hosaka M, Sugi M (1999) A simulation of troposphere, stratosphere and mesosphere with an MRI/JMA98 GCM. Pap Meteorol Geophys 50:15–53

Shindell DT, Grewe V (2002) Separating the influence of halogen and climate changes on ozone recovery in the upper stratosphere. J Geophys Res 107(D12): 4144. DOI 10.1029/2001JD000420

Shindell DT, Schmidt GA, Miller RL, Rind D (2001) Northern hemisphere winter climate response to greenhouse gas, volcanic, ozone and solar forcing. J Geophys Res 106:7193–7210

Sigmond M, Siegmund PC, Manzini E, Kelder H (2004) A simulation of the separate climate effects of middle atmospheric and tropospheric CO_2 doubling. J Clim 17(12):2352–2367

Steil B, Brühl C, Manzini E, Crutzen PJ, Lelieveld J, Rasch PJ, Roeckner E, Krüger K (2003) A new interactive chemistry-climate model: 1. Present-day climatology and interannual variability of the middle atmosphere using the model and 9 years of HALOE/UARS data. J Geophys Res 108(D9):4290. DOI 10.1029/2002JD002971

Swinbank R, O'Neill A (1994) A stratosphere-troposphere data assimilation system. Mon Weather Rev 122:686–702

Taylor CP, Bourqui MS (2005) A new fast stratospheric ozone chemistry scheme in an intermediate general-circulation model. I: description and evaluation. Q J R Meteorol Soc 131:2225–2242

Thompson DWJ, Solomon S (2005) Recent stratospheric climate trends as evidenced in radiosonde data: global structure and tropospheric linkages. J Clim 18:4785–4795

Warner CD, McIntyre ME (1999) Toward an ultra-simple spectral gravity wave parameterization for general circulation models. Earth Planet Space 51(7–8):475–484

Williamson DL (1997) Climate simulation with a spectral, semi-Lagrangian model with linear grids. In: Lin C, Laprise R, Ritchie H (eds) Numerical methods in atmospheric and ocean modelling: the Andre J Robert memorial volume. Can Meteorol and Oceangr Soc, Ottawa, pp 279–292

WMO (1999) Scientific assessment of ozone depletion 1998. Global ozone research and monitoring Project Rep 47

Yukimoto S, Noda A, Kitoh A, Sugi M, Kitamura Y, Hosaka M, Shibata K, Maeda S, Uchiyama T (2001) A new Meteorological Research Institute coupled GCM (MRI-CGCM2): model climate and its variability. Pap Meteorol Geophys 51:47–88

Yulaeva E, Holton JR, Wallace JM (1994) On the cause of the annual cycle in tropical lower-stratospheric temperatures. J Atmos Sci 51:169–174